Electronic Supplementary Material (ESI) for Journal of Materials Chemistry C.

Deep-blue fluorescent emitter based on 9,9-dioctylfluorene-bridge with a hybridized local and charge-transfer excited state for organic Light-Emitting Devices with EQE exceeding 8%

Xing Liu [a ξ], Wen Liu [a ξ], Dongyu Wu [b], Xiaozhen Wei [a], Long Wang [a], Hua Wang [a], Yanqin Miao [a*], Huixia Xu [a], Junsheng Yu [c], Bingshe Xu [a*]*

Contents

SI-2. Structure characteristics

1.Thermal properties

The thermal stabilities were investigated by TGA and DSC under a nitrogen atmosphere. As shown in Fig. S1, the material **TPA-DFCP** performed obvious thermal stability with decomposition temperature (T_d) of 398 ℃, and glass transition temperature (Tg) could not be observed, which is originated from the rigid frameworks of the fluorene. The excellent thermal stability of TPA-DFCP is beneficial to the application in OLEDs.

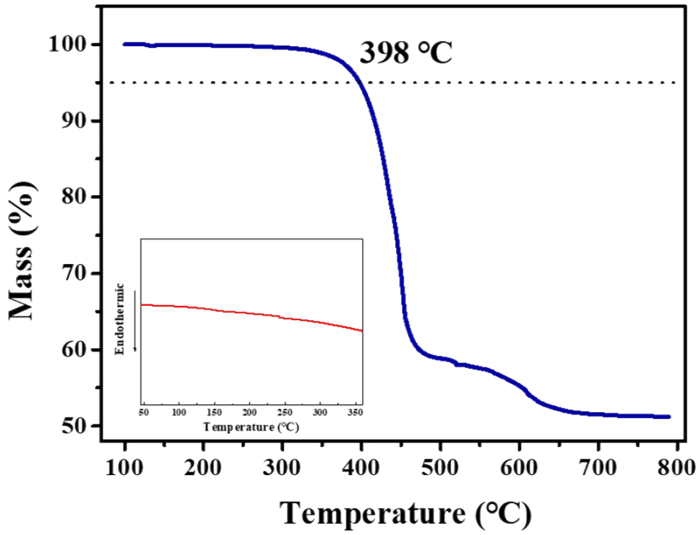

Fig. S1 TGA curve and DSC curve of **TPA-DFCP**.

2.electrochemical properties

The electrochemical cyclic voltammetry (CV) curve was measured to obtain the HOMO and LUMO energy levels of **TPA-DFCP** using ferrocene as an internal standard (Fig. S2). As shown, the oxidation peak of ferrocene located at 0.484 V (E_f^{ox}), and the oxidation peak of **TPA-DFCP** located at 0.914 V (E_c^{ox}). According to the formula E_{HOMO} = - [4.8 + (E_c^{ox} - E_f^{ox})] eV, the HOMO energy level can be calculated to be -5.284 eV. Meanwhile, the electrochemical bandgap (E_g) can be calculated to be 2.97 eV through the formula E_g=1240/λ. Over here, λ means the intersection of the absorption peak and emission peak of the film as 417 nm. Therefore, the LUMO energy level can be calculated to be -2.31 eV through the formula E_{LUMO} = E_{HOMO} + E_g.

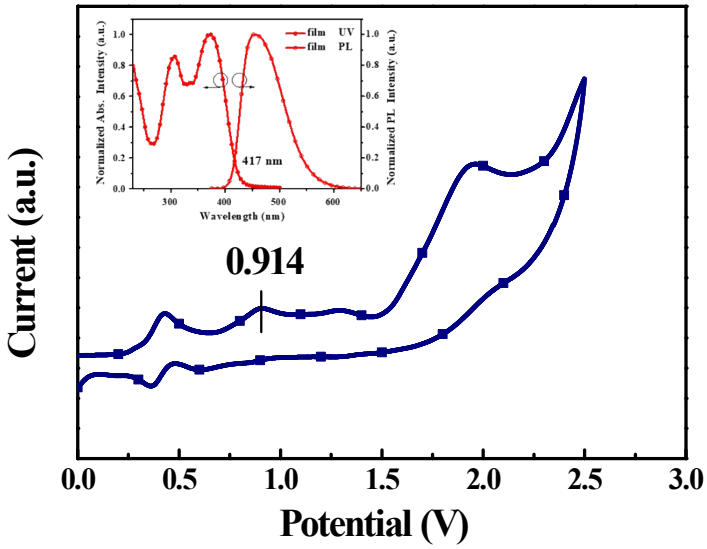

Fig. S2 cyclic voltammograms curve of **TPA-DFCP**

SI-3. Photophysical Properties

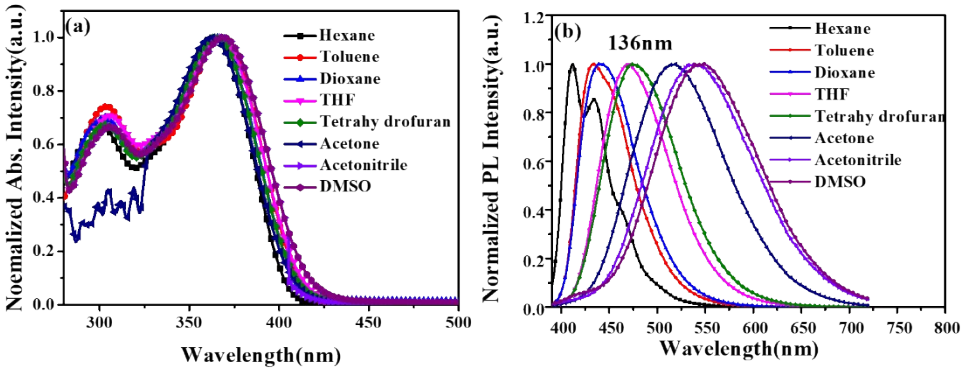

Fig. S3 UV-vis absorbance (a) and PL spectra (b) of **TPA-DFCP** in different polar solvents

1. Lippert-Mataga calculation

The ground-state dipole moment (μg) of TPA-DFCP were estimated to be 5.11 Debye through DFT at the level of B3LYP/6-31G (d, p). According to Lippert-Mataga equation (1) as introduced in previously reported works, the dipole moment of S_1 state ($\boldsymbol{\mu_e}$) was estimated.

$$hc(v_a - v_f) = hc(v_a^0 - v_f^0) + \frac{2(\mu_e - \mu_g)^2}{\alpha_0^3} f(\varepsilon,n) \quad (1)$$

Herein, ***h*** is Planck constant as $6.62*10^{-34}$ J/s, ***c*** is speed of light as $3*10^8$ m/s, ***f (ε, n)*** is the solvent polarity factor, $\boldsymbol{\nu_a}$-$\boldsymbol{\nu_f}$ is the stokes shift, $\boldsymbol{\nu_a^0}$-$\boldsymbol{\nu_f^0}$ is the stokes shift with ***f*** = 0, $\boldsymbol{\alpha_0}$ is the Onsager radius of the molecule. And, the $\boldsymbol{\mu_e}$ of TPA-DFCP in low polarity solvents is 6.36 D, and the $\boldsymbol{\mu_e}$ of TPA-DFCP in high polarity solvents is 31.76 D.

Table S1 Photophysical data of **TPA-DFCP** in different solvents.

Solvent	$f(\varepsilon,n)$	λ_{abs} (nm)	λ_{pl} (nm)	ν_a-ν_f (cm^{-1})
Hexane	0.0012	363	412	3276
Benzene	0.0026	367	435	4259
Toluene	0.012	368	433	4079
Dioxane	0.021	365	441	4721
Triethylamine	0.048	364	430	4216
Butyl Ether	0.096	364	433	4377
Chloromethane	0.149	367	471	6016
Ethyl ether	0.167	361	448	5379
Ethyl acetate	0.2	362	470	6347
Tetrahydrofuran	0.21	364	473	6330
Dichloromethane	0.217	365	493	7113
Dimethyl sulfoxide	0.2632	368	543	8757
Dimethyl formamide	0.276	367	536	8591
Acetone	0.28	362	519	8356
Acetonitrile	0.305	361	538	9113

2. Lifetime of the TPA-DFCP in film and different polar solutions

Fig. S4. Transient PL decay spectra of **TPA-DFCP** in film (a) and in different solvents (b)

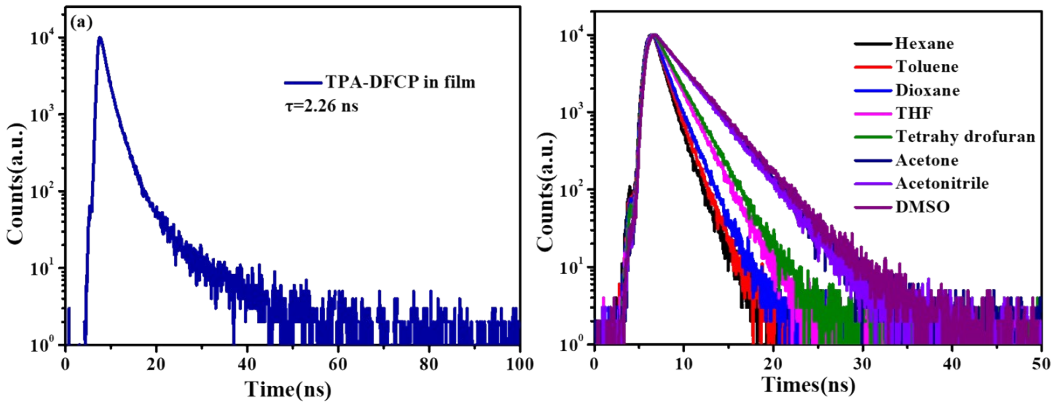

Table S2. Lifetime (**τ**) values of **TPA-DFCP** in different solvents and in film.

solution	**τ** (ns)	solution	**τ** (ns)	solution	**τ** (ns)
Hexane	1.20	Chloroform	1.89	Acetonitrile	3.02
Toluene	1.35	Tetrahydrofuran	2.13	Dimethyl sulfoxide	3.22
Dioxane	1.44	Acetone	3.09	film	2.26

3. PL spectra at room temperature and phosphorescence spectra

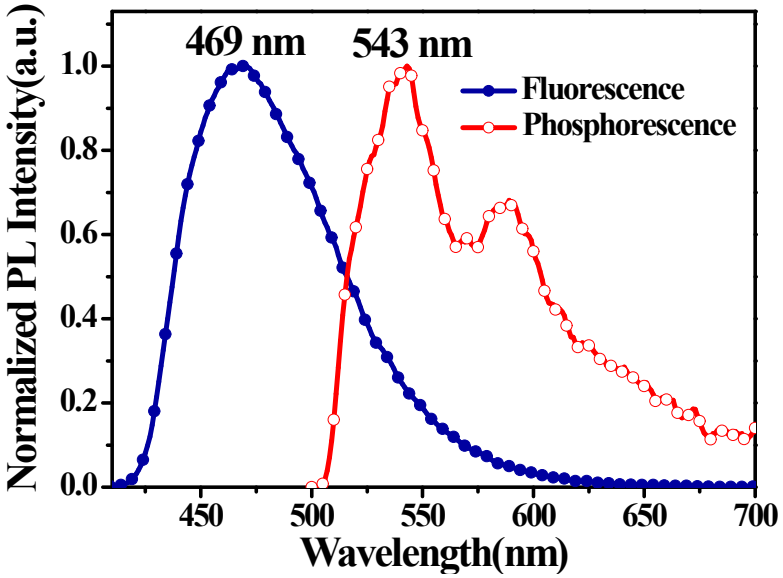

Fig. S5. PL spectra at room temperature and phosphorescence spectra (delayed by 0.256ms) of **TPA-DFCP** in toluene at 77K.

SI-4. Electroluminescent Performance

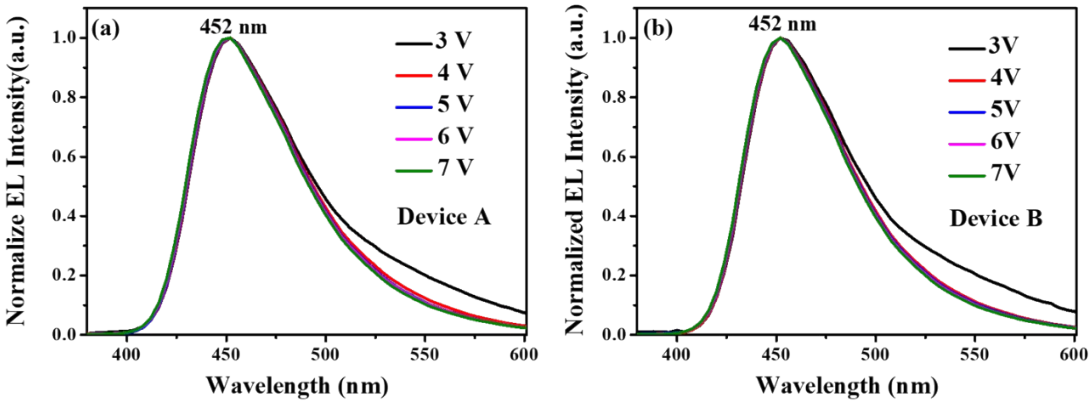

Fig. S6 Normalized EL spectra of the non-doped devices from 3 V to 7 V.

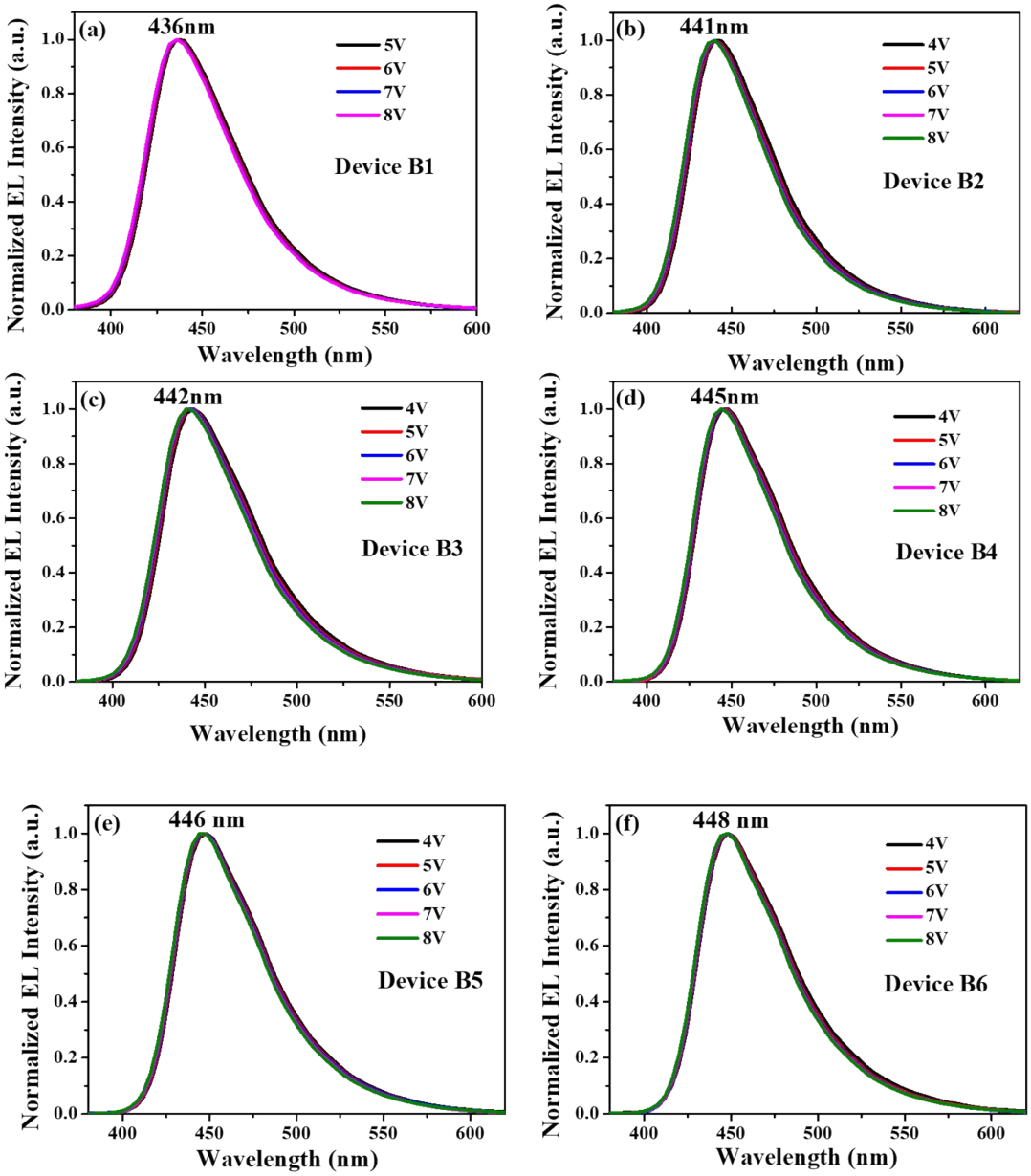

Fig. S7 Normalized EL spectra of the doped devices from 4 V to 8 V.

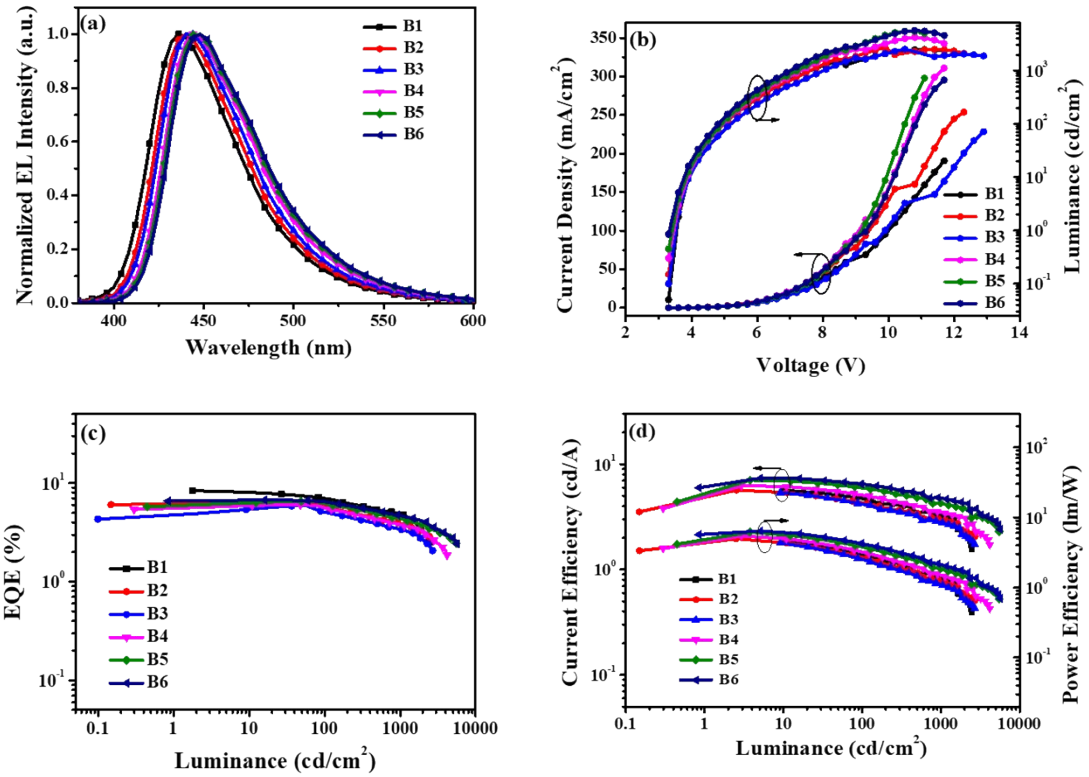

Fig. S8 EL performance of Device B1-B6: (a) EL spectra; (b) J-V-L curve; (c) CE-L-PE curve; (d) EQE-L curve.

Table S3. EL performance of devices based **TPA-DFCP**

TPA-DFCP	**doping ratio** (%)	λ_{EL} (nm)	CIE (x,y)	EQE_{max} [a] (%)	CE_{max} [b] (cd/A)	PE_{max} [c] (lm/W)	L_{max} [d] (cd/m^2)	V_{on} (V)
Device B1	5	436	(0.153,0.077)	8.30	5.63	4.87	2482	3.54
Device B2	10	441	(0.153, 0.084)	7.46	5.66	4.94	2509	3.59
Device B3	15	442	(0.152, 0.092)	6.52	5.35	4.61	2697	3.53
Device B4	30	445	(0.152, 0.104)	6.78	6.24	5.45	4194	3.44
Device B5	50	446	(0.152, 0.111)	7.21	7.05	6.15	5497	3.40
Device B6	80	447	(0.153, 0.117)	7.24	7.35	6.42	5660	3.31

[a] The maximum external quantum efficiency; [b] The maximum current efficiency; [c] The maximum power efficiency; [d] The maximum luminance; [e] The exciton utilization

SI-5. Synthesis

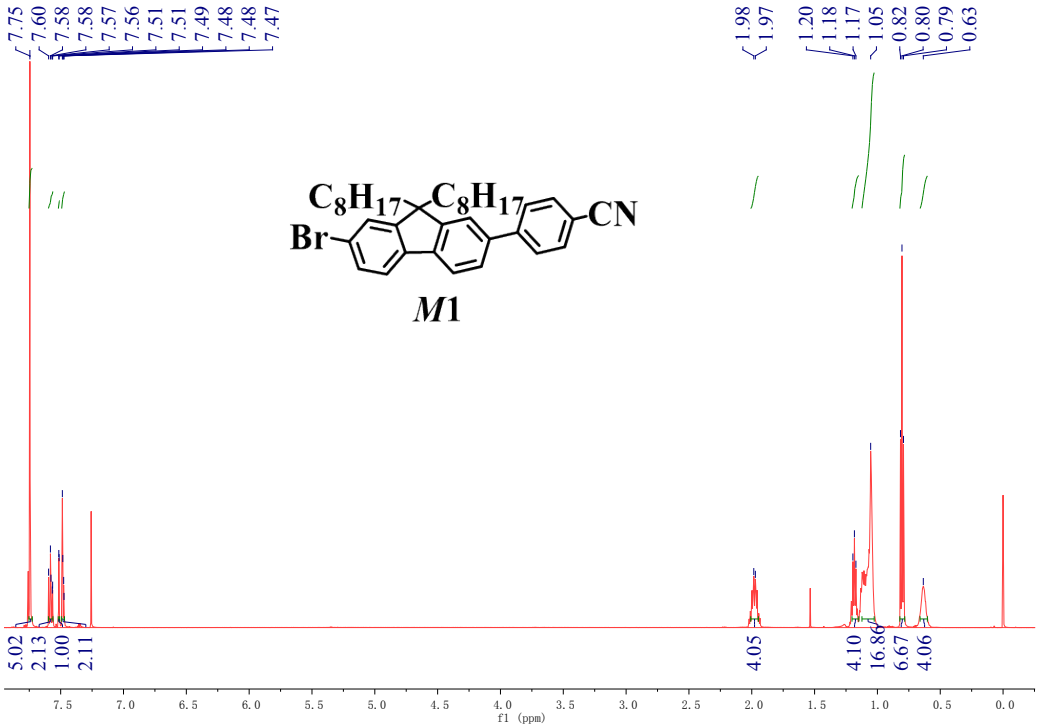

Fig. S9 ^{1}H NMR spectrum of ***M*1** in $CDCl_3$

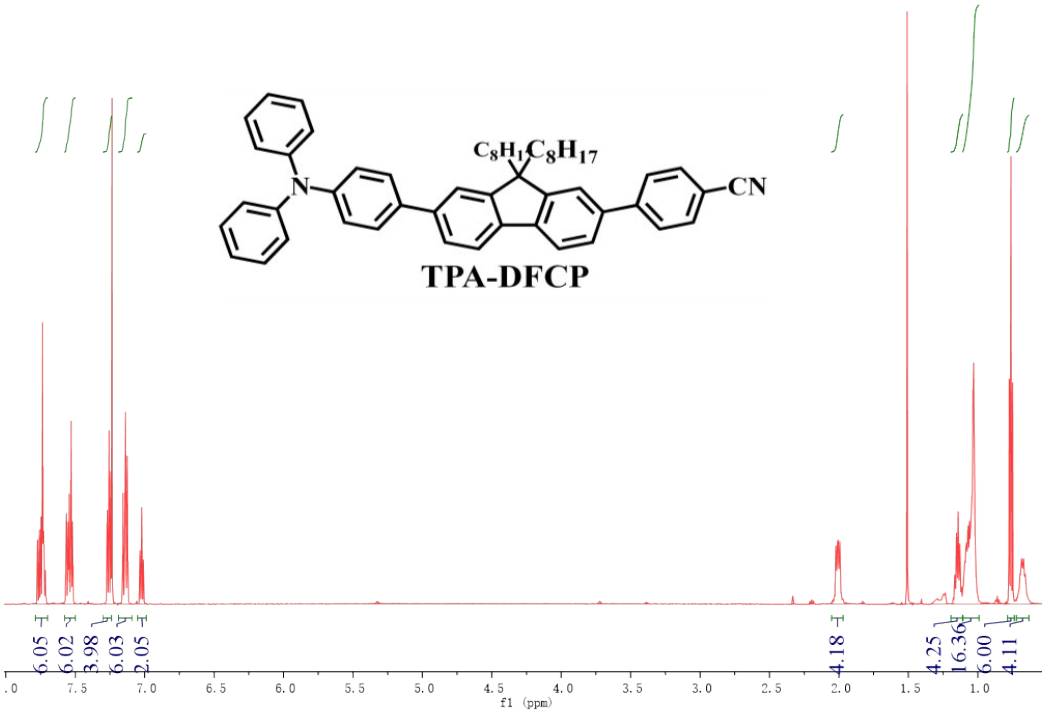

Fig. S10 ^{1}H NMR spectrum of **TPA-DFCP** in $CDCl_3$

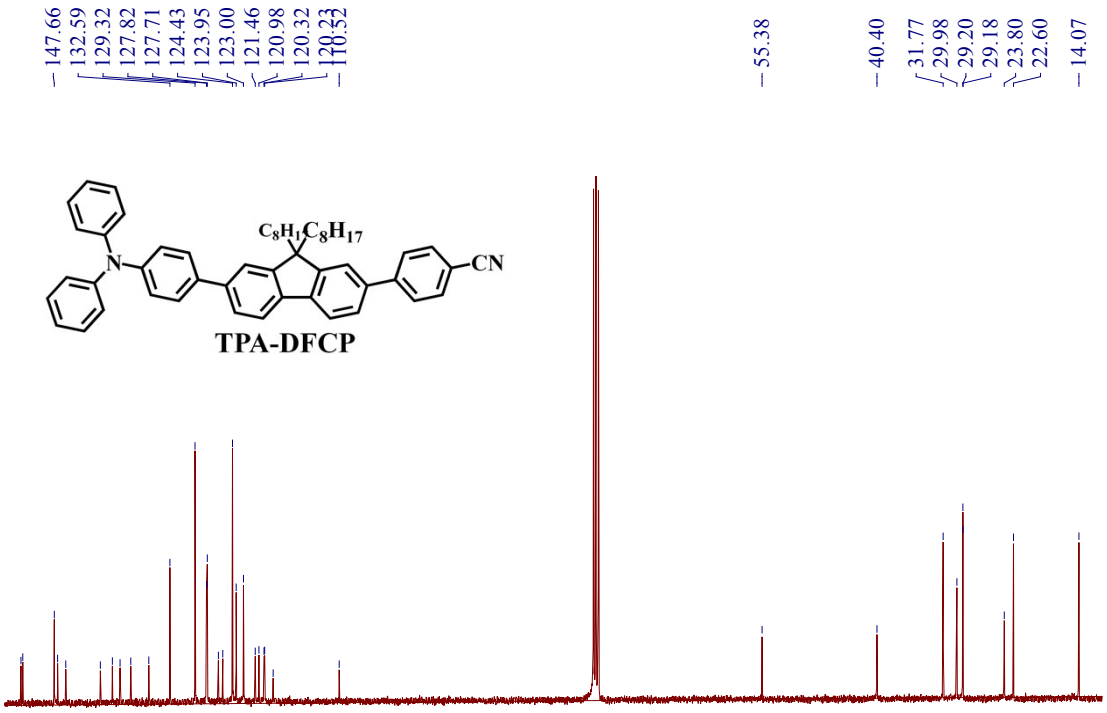

Fig. S11 ^{13}C NMR spectrum of **TPA-DFCP** in $CDCl_3$